J Fluoresc (2015) 25:1109–1115
DOI 10.1007/s10895-015-1601-6

ORIGINAL ARTICLE

Interaction of Anthracycline 3′-azido-epirubicin with Calf Thymus DNA via Spectral and Molecular Modeling Techniques

Fengling Cui[1] · **Xiaoqing Niu**[1] · **Luyao Li**[1] · **Pengge Zhang**[1] · **Guisheng Zhang**[1]

Received: 26 March 2015 / Accepted: 15 June 2015 / Published online: 25 June 2015

Abstract Anthracycline antibiotics are extensively applied to clinical antitumor therapy. The binding mode and mechanism of a new anthracycline 3′-azido-epirubicin (AEPI) with calf thymus deoxyribonucleic acid (ctDNA) were investigated employing multiple spectroscopy techniques in Tris-HCl buffer solution (pH 7.4). Effect of pH on the interaction was provided to determine the proper environment for whole research. Iodide quenching studies and fluorescence polarization measurement indicated that ctDNA quenched the fluorescence of AEPI significantly via intercalation binding mode. The binding constants and binding sites for the interaction were calculated. From binding constant dependence on the temperature, static quenching mechanism of AEPI by ctDNA was confirmed based on the Stern-Volmer equation. Additionally, the thermodynamic parameters for the reaction revealed that the van der Waals force and hydrogen bonding were the main acting forces in the binding process. Molecular modeling result indicated that the hydrogen bonding played a major role in the binding of AEPI to ctDNA.

Keywords 3′-azido-epirubicin · DNA · Interaction

Introduction

Anthracyclines from both natural and semisynthetic sources are among the most widely used chemotherapeutic agents and are effective in clinic against a broad spectrum of solid tumors and leukemias [1]. A class of anthracycline drugs with plane aromatic structure, for instance, doxorubicin, daunorubicin and epirubicin, have remarkable antitumor curative effect. Plane aromatic structure of the drugs intercalates into the base pairs of DNA, thus damages DNA template via hindering DNA replication and RNA transcription and then inhibiting the proliferation of cancer cells to obtain the aim of antitumor [2, 3]. However, the use of anthracyclines is considered as a double-edged sword. The following cardiotoxicity and drug resistance restrict their use in clinic enormously, although anthracyclines play an undisputed key role in the treatment of many neoplastic diseases [4]. The side effects have been attributed to the toxicity of these drugs toward mitochondria, leading to disturbance of bioenergetics, inhibitions of enzymes, oxidation of lipids, disorders of membrane, and oxidative stress [5]. Consequently, researchers are trying continuously to synthesize new classes of anthracycline drugs to enhance effective killing of tumor cells with less cardiotoxicity by structure modification and transformation, which may provide potential clinical use in the future.

Deoxyribonucleic acid (DNA) is an important genetic substance in organisms [6] and the main cellular target for studies with small molecules of biological importance such as carcinogens, steroids, and several classes of drugs [7]. Studies on binding mechanism contribute to understanding the mutation of genes and the origin of some diseases [8]. Binding of small molecules to DNA occurs primarily through three modes: electrostatic interactions, groove binding interactions, and intercalation into the stacked base pairs of native DNA [9]. Studying the interaction of DNA with small molecules, especially drug molecules, is an important task in many research fields such as medicinal chemistry, life science, clinical medicine, and so on [10]. Through investigating the binding mode and effective mechanism of drugs with DNA, scientific

✉ Fengling Cui
fenglingcui@hotmail.com

[1] College of Chemistry and Chemical Engineering, Key Laboratory of Green Chemical Media and Reactions, Ministry of Education, Henan Normal University, Xinxiang 453007, China

theoretical information can be provided for the rational design and construction of new and more efficient drugs with lower toxicity.

Epirubicin, a stereoisomer of doxorubicin, favored over doxorubicin due to more therapeutic index and lesser side effects [11, 12]. Besides, it is often used for the treatment of non Hodgkin lymphoma and breast cancer in conjunction with other drugs [13, 14]. In this work, we studied the interaction of an analog of epirubicin, a novel anthracycline AEPI (shown in Fig. 1), with ctDNA using fluorescence spectroscopy, iodide quenching, fluorescence polarization and molecular modeling under simulated physiological conditions. The quenching mechanism and binding mode were clarified. Furthermore, we explored the dominant interaction forces, binding constant and binding sites for the interaction of AEPI with ctDNA.

Experimental Section

Materials

ctDNA was obtained from Sigma-Aldrich Company (USA). ctDNA stock solution was obtained by dissolving the solid ctDNA directly in the double-distilled water without further purification and stored at 0~4 °C in the dark. The purity of ctDNA was confirmed via the UV ratio of absorbance at 260/280 nm. The ratio A_{260}/A_{280}>1.8 indicated that ctDNA was free from protein fully. The concentration of ctDNA stock solution was calculated according to the absorbance at 260 nm using a molar absorption coefficient of 6600 $L \cdot mol^{-1} \cdot cm^{-1}$. AEPI solution ($1.16 \times 10^{-4}$ $mol \cdot L^{-1}$) was prepared in N,N-dimethylformamide. Tris-HCl solution (pH 7.4) and KI solution (2×10^{-2} $mol \cdot L^{-1}$) were prepared. All reagents were of analytical grade and double-distilled water was used throughout.

Apparatus

The pH measurements were determined with a PFS-80 pF-meter (Shanghai Dazhong Analytical Instrument Plant, Shanghai, China). Fluorescence spectra were measured with a Cary Eclipse fluorescence spectrophotometer (VARIAN, USA) using a 1 cm quartz cuvette. Both the excitation and emission slit widths were set to 5 nm. A SHP DC-0515 thermostatic water bath (Shanghai Hengping Sciences Instrument Co. Ltd., Shanghai, China) was used for controlling the temperature. The absorption measurements were performed with a Tu-1810 double beam spectrophotometer (Beijing General Instrument, China) using a 1.0 cm cell.

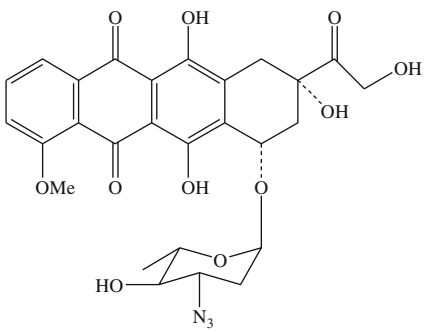

Fig. 1 Structure of AEPI ($C_{27}H_{27}N_3O_{11}$, molecular weight 569)

Procedures

Effect of pH

A certain amount of AEPI and ctDNA and 2 mL different pH value buffer solution were added to 10 mL volumetric flask, and diluted with double distilled water. The emission spectra were recorded on a Varian Cary Eclipse spectrofluorimeter coupled with a 1.0 cm path length fluorescence cuvette.

Fluorescence Spectra

Two milliliters pH 7.4 Tris-HCl buffer solution, a certain amount of AEPI and various amounts of ctDNA were diluted with double distilled water to 10 mL volumetric flask. The emission spectra were recorded from 520 to 720 nm with excitation wavelength 253 nm at 301, 310 and 320 K.

Iodide-Quenching Studies

Potassium iodide was used as the quencher for iodide quenching studies. A series of assay solutions containing various amounts of KI and a fixed amount of AEPI and AEPI-ctDNA were prepared to measure the fluorescence intensity.

Fluorescence Polarization

Two milliliters pH 7.4 Tris-HCl buffer solution was added to a series of 10 mL volumetric flask. Then added a certain amount of AEPI and increasing concentration of ctDNA and diluted with double distilled water. The fluorescence polarization measurements were performed on the maximum excitation and emission wavelengths with excitation and emission slit widths at 10 nm.

Molecular Modeling

The binding model between AEPI and ctDNA was generated by Sybyl 6.9. The geometry of AEPI was optimized using the Tripos force field with Gasteiger-Huckel charges in the Sybyl 6.9 suite. The crystal structure of DNA used for docking was extracted from the Protein Data Bank identifier 453D. Before docking run, water was removed from the DNA PDB file and essential polar hydrogen atoms and Gasteiger charges were added. A maximum of 10 conformers were considered for

the ligand. The conformer with the lowest binding free energy was used for further analysis. During the docking process, rotatable bonds in the ligand were assigned with FlexX. The radius around the solvent molecules was set to 12 Å. DNA was enclosed in a grid having 0.375 Å spacing. Other miscellaneous parameters were set as default.

Results and Discussion

Effect of pH Value

As to DNA, the environmental pH plays an influential role in its stability of double-stranded structures [15]. Thus, in our study, the effect of different pH buffer solution on the interaction of ctDNA with AEPI has been investigated under the fixed concentration of ctDNA and AEPI. From Fig. 2, it can be concluded that the fluorescence intensity of ctDNA-AEPI system changes remarkably with pH. The fluorescence intensity of the system is gradually increasing in relatively small extent with pH value in the range of 5~7.4 while it reduces drastically when pH value is above 7.8. The results demonstrate that strong acid or alkaline condition has adverse effects on the binding of AEPI with ctDNA. Hence, the buffer solution of pH 7.4 near neuter is chosen for the whole experiment.

Fluorescence Characteristic of ctDNA Interaction with AEPI

Quenching Mechanism

Figure 3 displays the fluorescence quenching spectra of ctDNA-AEPI system. When the excitation wavelength was set to 253 nm, a maximum emission peak at 595 nm was observed in the emission spectra. And with increasing concentration of ctDNA, the fluorescence intensity of AEPI at around 595 nm regularly decreased. Besides, the shape of the fluorescence spectra was not changed. The results suggested AEPI could strongly interact with ctDNA through noncovalent bond.

Fluorescence quenching is the process of fluorescence intensity reduced due to the interactions of luminophore with other substances. These interactions include excited state intermolecular interaction, molecular rearrangement, energy transfer, complex formation, molecule collision, etc. [16]. There are two main types of quenching mechanism: static

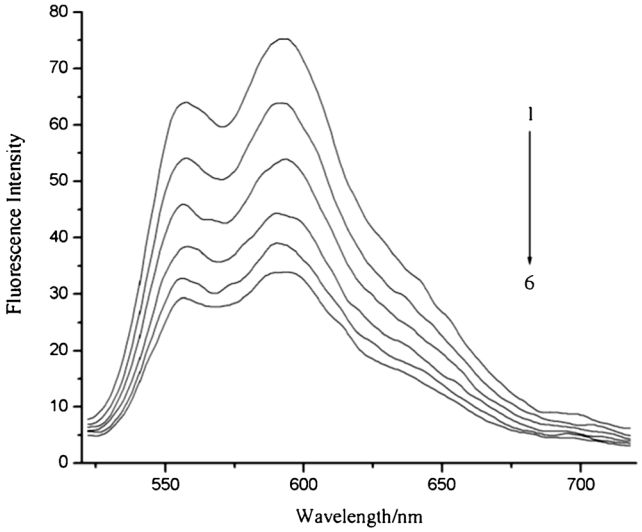

Fig. 3 Fluorescence emission spectra of AEPI in the presence of different DNA concentrations. Conditions: $C_{AEPI}=3.48\times10^{-6}$ mol·L^{-1}; from 1 to 6, C_{ctDNA} =0, 9.76, 19.52, 29.28, 39.04, 48.80$\times10^{-6}$ mol·L^{-1}

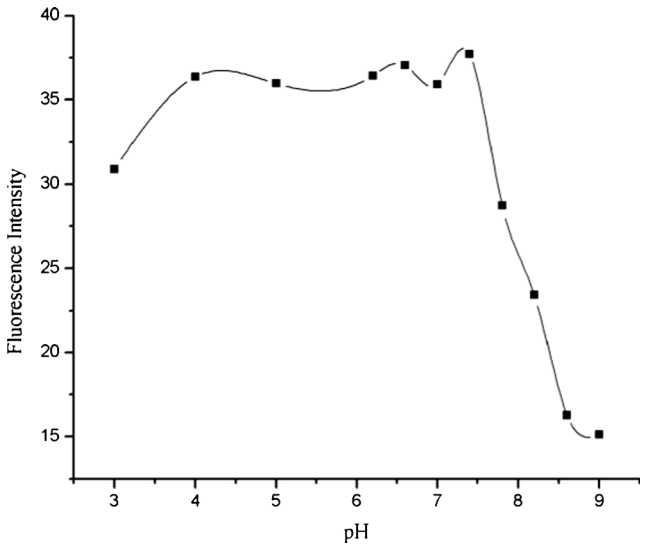

Fig. 2 Effect of different pH on the ctDNA-AEPI system. Conditions: $C_{AEPI}=2.32\times10^{-6}$ mol·L^{-1}; $C_{ctDNA}=9.76\times10^{-6}$ mol·L^{-1}

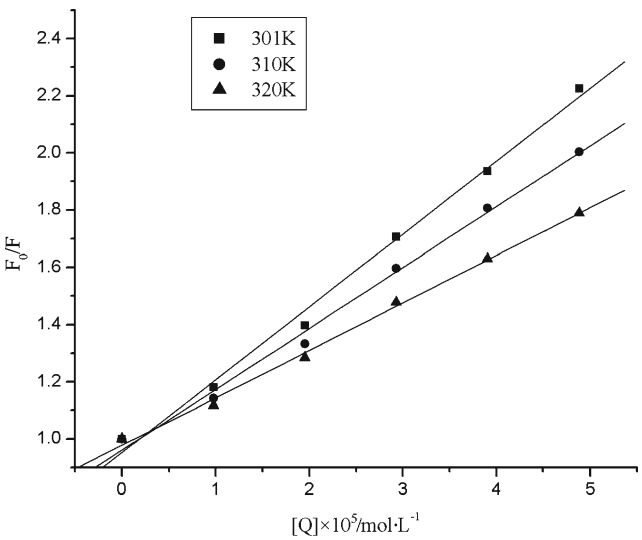

Fig. 4 Stern-Volmer curves for the fluorescence quenching of AEPI by ctDNA at 301, 310 and 320 K

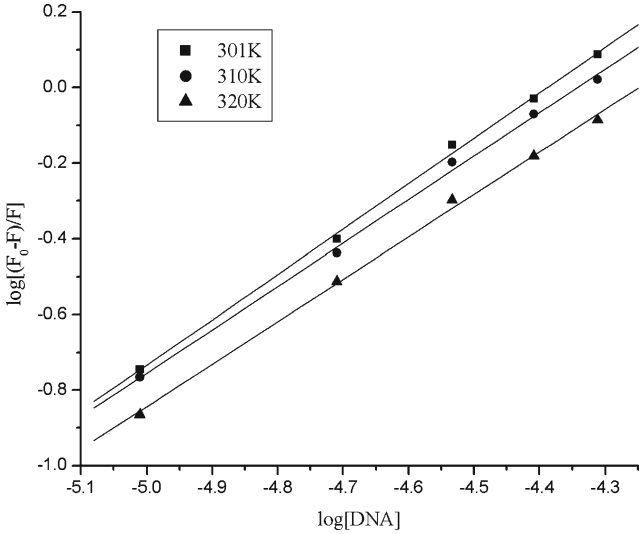

Fig. 5 The plot of log[(F_0-F)/F] versus log[Q] at different temperatures

and dynamic quenching [17]. Dynamic quenching is closely related to the degree of molecular diffusion, thereby the quenching constant increases as the temperature goes up. However, the quenching constant of static quenching process has the reverse effect with increasing temperature [18]. The fluorescence data are analysed based on the Stern-Volmer equation [19]:

$$F_0/F = 1 + K_q\tau_0[Q] = 1 + K_{SV}[Q] \quad (1)$$

where F_0 and F denote the fluorescence intensities in the absence and presence of ctDNA, respectively. K_{SV} is the Stern-Volmer quenching constant. [Q] is the concentration of ctDNA. τ_0 is the fluorescence life time in the absence of ctDNA and K_q is the quenching constant of biomacromolecule. A plot of F_0/F against [Q] at different temperatures is shown in Fig. 4. These slopes (K_{SV}) are found to be 2.54×10^4, 2.13×10^4 and 1.66×10^4 L·mol^{-1} at 301, 310 and 320 K, respectively. It is apparent that the value of K_{SV} is inversely correlated with temperature, which provides direct evidence that the fluorescence quenching is the consequence of static quenching instead of dynamic collision quenching. Meanwhile, the corresponding values of K_q at three temperatures are calculated to be 2.54×10^{12}, 2.11×10^{12}, and 1.65×10^{12} L·mol^{-1}·s^{-1}, respectively. These values are all greater than 2×10^{10} L·mol^{-1}·s^{-1}, the maximum diffusion collision quenching rate constant of biopolymers by quenchers [20], which is the further proof that the quenching mechanism is static quenching.

Binding Constants and Binding Forces

The binding constant K and the number of binding sites n were obtained by double-logarithm regression equation [21]:

$$\log\frac{F_0-F}{F} = \log K + n\log[Q] \quad (2)$$

where F_0 and F are the emission intensities of AEPI in the absence and presence of ctDNA, respectively. Figure 5 shows the double-logarithm curve and the values of K and n are listed in Table 1. Based on the data in Table 1, the high values of the binding constants indicate that AEPI binds to ctDNA with high affinity. The values of n approximately equal to 1 manifest the existence of only one binding site of AEPI with ctDNA.

Small molecules form complexes with biomacromolecules, such as DNA and protein, mainly through four forces: electrostatic force, van der Waals force, hydrophobic interaction, hydrogen bonding, etc [22]. The thermodynamic parameters, free energy change (ΔG), enthalpy change (ΔH), and entropy change (ΔS) of the binding reaction can provide evidence for clarifying interaction modes. Binding forces of the interaction can be confirmed according to the thermodynamic parameters from the van't Hoff equation:

$$\ln K = -\Delta H/RT + \Delta S/R \quad (3)$$

$$\Delta G = \Delta H - T\Delta S \quad (4)$$

where K is the binding constant at corresponding temperature, and R is the gas constant. The temperatures are 301, 310 and 320 K, respectively. ΔH and ΔS are obtained from the slope and intercept of the plot of ln$K$ vs. $1/T$ (in Fig. 6). Furthermore, values of ΔG are calculated and the results are listed in Table 1.

Table 1 The binding constants and the thermodynamic paramenters of the interaction between AEPI and ctDNA at different temperatures

Temperature/K	K/ L·mol^{-1}	n	ΔG/kJ·mol^{-1}	ΔH/kJ·mol^{-1}	ΔS/J·mol^{-1}·k^{-1}
301	1.85×10^5	1.20	−30.27		
310	0.97×10^5	1.15	−29.70	−49.38	−63.48
320	0.59×10^5	1.12	−29.07		

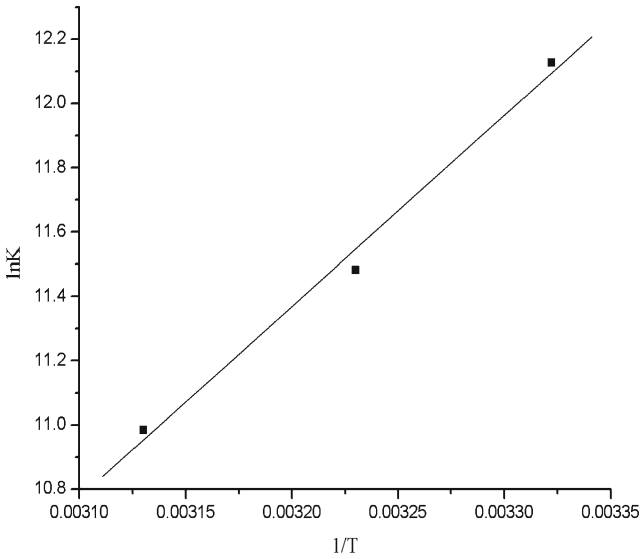

Fig. 6 Van 't Hoff plot of ctDNA-AEPI system

The negative value of ΔG suggests the spontaneity of the interaction. The negative value of ΔH shows that AEPI binding to ctDNA is exothermic, which is consistent with the negative correlation between binding constants and temperatures. Generally, the negative ΔH and the positive ΔS signify electrostatic force dominates the reaction, the negative ΔH and ΔS imply hydrogen bonding and van der Waals force play the main role, and the positive ΔH and ΔS point out hydrophobic interaction as the major interaction force [18, 23]. Consequently, we conclude that the interaction of AEPI binding to ctDNA was mainly driven by hydrogen bonding and van der Waals force.

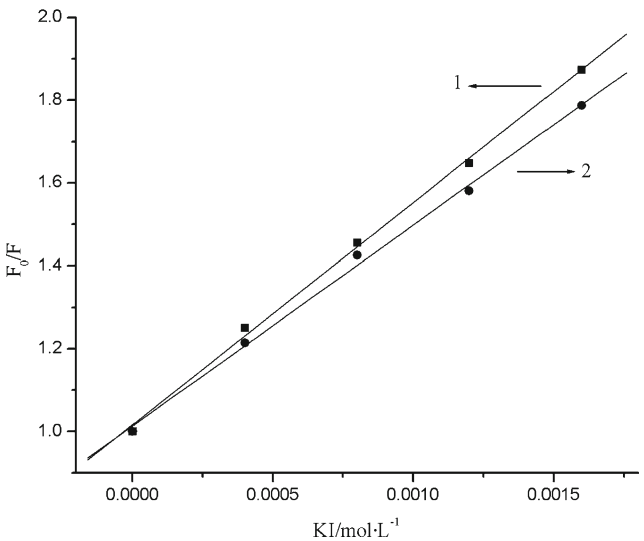

Fig. 7 Fluorescence quenching plot of AEPI by KI in the absence (line 1) and presence (line 2) of ctDNA. Conditions: $C_{AEPI}=2.32\times10^{-6}$ mol·L^{-1}; $C_{ctDNA}=9.76\times10^{-6}$ mol·L^{-1}

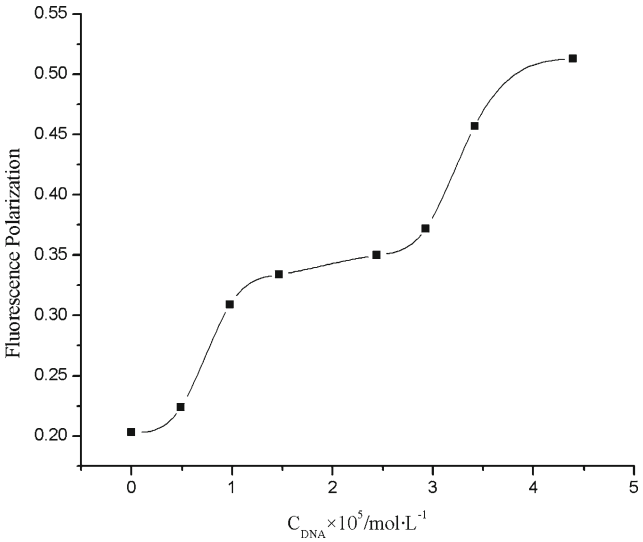

Fig. 8 Effect of ctDNA concentrations on the fluorescence polarization of AEPI. Conditions: $C_{AEPI}=2.32\times10^{-6}$ mol·L^{-1}; $C_{ctDNA}=0$, 0.488, 0.976, 1.464, 2.440, 2.928, 3.416, 4.392×10^{-5} mol·L^{-1}

Determination of Binding Mode of ctDNA-AEPI System

Iodide Quenching Studies

Supposing that small molecules bind to DNA through surface-binding mode, which cannot afford a protection surrounding for the small molecule, the collision probability between small molecule and anionic quenchers with the presence and

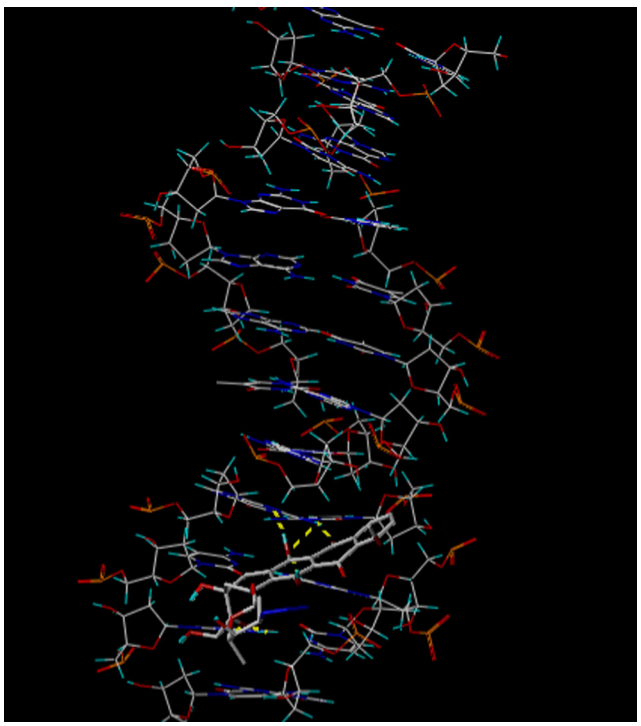

Fig. 9 Molecular modeling of AEPI intercalating to ctDNA with preference of the G-C rich region

absence of DNA will be equal [24]. When small molecules intercalate into the DNA base pairs, the double helix structure of DNA will protect the molecules from binding to anionic quenchers owing to the electrostatic repelling, thus the magnitude of K_{SV} of bound molecules was lower than that of free molecules [25]. On the contrary, if small molecules interact with DNA through groove binding, then only part of them are protected by DNA, and anionic quenchers could quench the fluorescence of small molecules to some extent [26]. As a result, the magnitude of K_{SV} of bound molecules was higher than that of free molecules.

Potassium iodide could quench the fluorescence of small molecules effectively, and exclude DNA phosphate backbone with negative charges as well. Therefore, it is chosen as anionic quenching agent for the experiment to deduce the binding mode of the interaction from the variation of K_{SV}. According to Stern-Volmer equation, fluorescence quenching plot is exhibited in Fig. 7. From the slope of Stern-Volmer curve, we obtain that the quenching constants of AEPI and AEPI-ctDNA by KI are 610 and 565 $L \cdot mol^{-1}$, respectively. Obviously, the quenching effect by KI is weaken when AEPI is bound to ctDNA, thereby proving that AEPI intercalates into ctDNA.

Fluorescence Polarization Measurement

As an important fluorescence parameter, fluorescence polarization provides surrounding microenvironment information of small molecules in the solution. In water solution, fluorescence polarization values decrease in virtue of small block level of rotation motion and fast rotation speed. However, if small molecules intercalate into the double helix structure of DNA, the rotation motion should be restricted, resulting in the increase of fluorescence polarization value. In contrast, when small molecules interact with DNA by electrostatic interaction or groove binding, fluorescence polarization has no obvious change [27]. The measurement of polarization based on the following equations [28]:

$$P = \frac{I_{VV} - GI_{VH}}{I_{VV} + GI_{VH}} \quad (5)$$

$$G = \frac{I_{HV}}{I_{HH}} \quad (6)$$

where I_{VV} is the vertical polarization intensity vertical with excitation; I_{VH} is the horizontal polarization intensity vertical with excitation; I_{HV} is the vertical polarization intensity parallel with excitation; I_{HH} is the horizontal polarization intensity parallel with excitation. The effect of different ctDNA concentrations on fluorescence polarization was measured and the result is given in Fig. 8. It is clear that the fluorescence polarization is weak in the absence of ctDNA. Meanwhile, with the increasing amounts of ctDNA, the fluorescence polarization gradually increases. The result corroborates the intercalating binding of AEPI to DNA, which further supports the conclusion from KI quenching experiment.

Molecular Modeling Studies

Generally, molecular modeling is widely used in the design of new drugs, as it may provide some insight into the interactions between the ligands and macromolecules [29]. FlexX program was applied to calculate the possible conformation of the ligands that binds to the ctDNA. The docked structure (Fig. 9) exhibited the optimal energy ranking results of AEPI binding to ctDNA. It suggested that the chromophore of AEPI could slide into the G-C rich region of ctDNA. As for AEPI, the H21 atom of G-10 were at a distance of 1.93 and 1.98 Å from carbonyl O atom and phenolic hydroxyl O atom, respectively. The H22 atom of G-10 was at a distance of 2.49 Å from phenolic hydroxyl O atom. Similarly, the O atom of C-15 was 2.08 Å from the hydroxy H atom. Molecular modeling study indicated that the interaction of AEPI with ctDNA was dominated by intercalation and hydrogen bonding forces played an essential role in the binding.

Conclusion

The present work reports the binding characteristic of AEPI with ctDNA. The fluorescence quenching mechanism of AEPI by ctDNA is static quenching. The binding mode of AEPI with ctDNA has been evidenced to be intercalative. The binding constants and the number of binding sites were measured at different temperatures. Concurrently, the hydrogen bonding and van der Waals force, the major interaction forces between AEPI and ctDNA, have also been discussed through thermodynamic equations. Moreover, the effect of pH on the binding was also investigated. Molecular modeling result was consistent with the experimental results. This work may provide the comparison on the efficacy of other anthracyclines interactions with DNA and the theoretical basis for new anthracycline design which will be valuable for clinical research.

Acknowledgments We gratefully acknowledge the financial support of National Natural Science Foundation of China (30970696, 21172056), Key Project of Henan Ministry of Education (14A150018), Key Programs of Henan for Science and Technology Development (142102310273), PCSIRT (IRT1061), and the Program for Innovative Research Team in University of Henan Province (2012IRTSTHN006).

References

1. Shaul P, Frenkel M, Goldstein EB, Mittelman L, Grunwald A, Ebenstein Y, Tsarfaty I, Fridma M (2013) The structure of anthracycline derivatives determines their subcellular localization and cytotoxic activity. ACS Med Chem Lett 4:323–328

2. Guina PS, Dasb S, Mandala PC (2009) Studies on the formation of a complex of Cu(II) with sodium 1,4-dihydroxy-9,10-anthraquinone-2-sulphonate – an analogue of the core unit of anthracycline anticancer drugs and its interaction with calf thymus DNA. J Inorg Biochem 103:1702–1710
3. Chaires JB, Dattagupta N, Crothers DM (1982) Studies on interaction of anthracycline antibiotics and deoxyribonucleic acid: equilibrium binding studies on interaction of daunomycin with deoxyribonucleic acid. Biochemistry 21:3933–3940
4. Minotti G, Menna P, Salvatorelli E, Cairo G, Gianni L (2004) Anthracyclines: molecular advances and pharmacologic developments in antitumor activity and cardiotoxicity. Pharmacol Rev 56: 185–229
5. Ming LJ (2003) Structure and function of "Metalloantibiotics". Med Res Rev 23:697–762
6. Denning EJ, MacKerell AD Jr (2011) Impact of arsenic/phosphorus substitution on the intrinsic conformational properties of the phosphodiester backbone of DNA investigated using ab initio quantum mechanical calculations. J Am Chem Soc 133:5770–5772
7. Zhang GW, Fu P, Wang L, Hu MM (2011) Molecular spectroscopic studies of farrerol interaction with calf thymus DNA. J Agric Food Chem 59:8944–8952
8. Kara HES (2014) Redox mechanism of anticancer drug idarubicin and in-situ evaluation of interaction with DNA using an electrochemical biosensor. Bioelectrochemistry 99:17–23
9. Erdem A, Ozsoz M (2001) Interaction of the anticancer drug epirubicin with DNA. Anal Chim Acta 437:107–114
10. Campbell NH, Smith DL, Reszka AP, Neidle S, O'Hagan D (2011) Fluorine in medicinal chemistry: β-fluorination of peripheral pyrrolidines attached to acridine ligands affects their interactions with G-quadruplex DNA. Org Biomol Chem 9:1328–1331
11. Arcamone F (1987) Clinically useful doxorubicin analogues. Cancer Treat Rev 14:159–161
12. Launchbury AP, Habboubi N (1993) Epirubicin and doxorubicin: a comparison of their characteristics, therapeutic activity and toxicity. Cancer Treat Rev 19:197–228
13. Coukell AJ, Faulds D (1997) Epirubicin. Drugs 53:453–482
14. Glück S (2005) Adjuvant chemotherapy for early breast cancer: optimal use of epirubicin. Oncologist 10:780–791
15. Wang YC, Lin CB, Su JJ, Ru YM, Wu Q, Chen ZB, Mao BW, Tian ZW (2011) Electrochemically-driven large amplitude pH cycling for acid–base driven DNA denaturation and renaturation. Anal Chem 83:4930–4935
16. Li GQ, Chen DB, Mo YM, Bai FL (1996) Studies on the fluorescence quenching of anthracenes by polysilane copolymers. J Appl Polym Sci 59:1463–1466
17. Shahabadi N, Heidari L (2014) Synthesis, characterization and multi-spectroscopic DNA interaction studies of a new platinum complex containing the drug metformin. Spectrochim Acta A 128:377–385
18. Ross PD, Subramanian S (1981) Thermodynamic of protein association reactions: forces contributing to stability. Biochemistry 20: 3096–3102
19. Khorasani-Motlagh M, Noroozifar M, Khmmarnia S (2011) Study on fluorescence and DNA-binding of praseodymium(III) complex containing 2,2′-bipyridine. Spectrochim Acta A 78:389–395
20. Zhang GW, Guo JB, Zhao N, Wang JR (2010) Study of interaction between kaempferol–Eu^{3+} complex and DNA with the use of the neutral red dye as a fluorescence probe. Sensors Actuators B 144: 239–246
21. Zhong W, Yu JS, Huang W, Ni K, Liang Y (2001) Spectroscopic studies of interaction of chlorobenzylidine with DNA. Biopolymers 62:315–323
22. Zhang LW, Wang K, Zhang XX (2007) Study of the interactions between fluoroquinolones and human serum albumin by affinity capillary electrophoresis and fluorescence method. Anal Chim Acta 603:101–110
23. Qiao CY, Bi SY, Sun Y, Song DQ, Zhang HQ, Zhou WH (2008) Study of interactions of anthraquinones with DNA using ethidium bromide as a fluorescence probe. Spectrochim Acta A 70:136–143
24. Xu M, Ma ZR, Huang L, Chen FJ, Zeng ZZ (2011) Spectroscopic studies on the interaction between Pr(III) complex of an ofloxacin derivative and bovine serum albumin or DNA. Spectrochim Acta A 78:503–511
25. Yang X, Liu WH, Jin WJ, Shen GL, Yu RQ (1999) DNA binding studies of a solvatochromic fluorescence probe 3-methoxybenzanthrone. Spectrochim Acta A 55:2719–2727
26. Dong C, Wei YX, Wei YL (2005) Study on the interaction between methylene violet and calf thymus DNA by molecular spectroscopy. J Photochem Photobiol A 174:15–22
27. Kumar CV, Asuncion EH (1993) DNA binding studies and site selective fluorescence sensitization of an anthryl probe. J Am Chem Soc 115:8547–8553
28. Guo LM, Dong WJ, Tong XF, Dong C, Shuang SM (2006) Study on spectroscopic characterization of Pd porphyrin and its interaction with ctDNA. Talanta 70:630–636
29. Żołek T, Maciejewska D (2010) Theoretical models of pentamidine analogs activity based on their DNA minor groove complexes. Eur J Med Chem 45:1991–1999